ISSN 1027-5495. Functional Materials, 28, No.3 (2021), p. 444-449.
doi:https://doi.org/10.15407/fm28.03.444

Kinetics of layer polymorphous crystallization of amorphous films of antimony sulfide

A.G.Bagmut

National Technical University "Kharkiv Politechnic Institute",
2, Kyrpychova Str., 61002 Kharkiv, Ukraine

Received March 29, 2021

Geometry and kinetics of crystal growth in amorphous films of antimony sulfide was studied by the methods of transmission electron microscopy *in situ* with video recording of structural changes. It was demonstrated, that electron-beam irradiation of an amorphous film with stoichiometric composition causes its layer polymorphous crystallization. In the area of the film heated by an electron beam, a single flat Sb_2S_3 crystal of an elliptical shape nucleates and grows. With a linear (in time t) increase in the crystal size, the crystallized fraction $x \sim t^2$, and the crystallization process is characterized by a relative length $\delta_0 \approx 4068$. In the case of a nonlinear increase in the crystal size $x \sim t^{1.2}$, the crystallization process is characterized by a relative length $\delta_0 \approx 2898$.

Keywords: amorphous state, kinetics, antimony sulfide, crystallization, electron microscopy, video recording.

Кінетика шарової поліморфної кристалізації аморфних плівок сульфіду сурми. *О.Г.Багмут*

Методами просвічувальної електронної мікроскопії *in situ* з відеозаписом структурних змін досліджено геометрію і кінетику росту кристалів в аморфних плівках сульфіду сурми. Показано, що опромінення електронним променем аморфної плівки стехіометричного складу викликає її шарову поліморфну кристалізацію. В області електронно-променевого нагріву плівки зароджується і зростає одиночний плоский еліпсоподібний кристал Sb_2S_3. При лінійному (за часом t) збільшенню розміру кристала частка закристалізованої речовини $x \sim t^2$, а процес кристалізації характеризується відносною довжиною $\delta_0 \approx 4068$. У разі нелінійного збільшення розміру кристала $x \sim t^{1.2}$, а процес кристалізації характеризується відносною довжиною $\delta_0 \approx 2898$.

Методами просвечивающей электронной микроскопии *in situ* с видеозаписью структурных изменений исследованы геометрия и кинетика роста кристаллов в аморфных пленках сульфида сурьмы. Показано, что облучение электронным пучком аморфной пленки стехиометрического состава вызывает ее слоевую полиморфную кристаллизацию. В области электронно-лучевого нагрева пленки зарождается и растет одиночный плоский эллипсовидный кристалл Sb_2S_3. При линейном (по времени t) увеличении размера кристалла доля закристаллизованного вещества $x \sim t^2$, процесс кристаллизации характеризуется относительной длиной $\delta_0 \approx 4068$. В случае нелинейного увеличения размера кристалла $x \sim t^{1.2}$, процесс кристаллизации характеризуется относительной длиной $\delta_0 \approx 2898$.

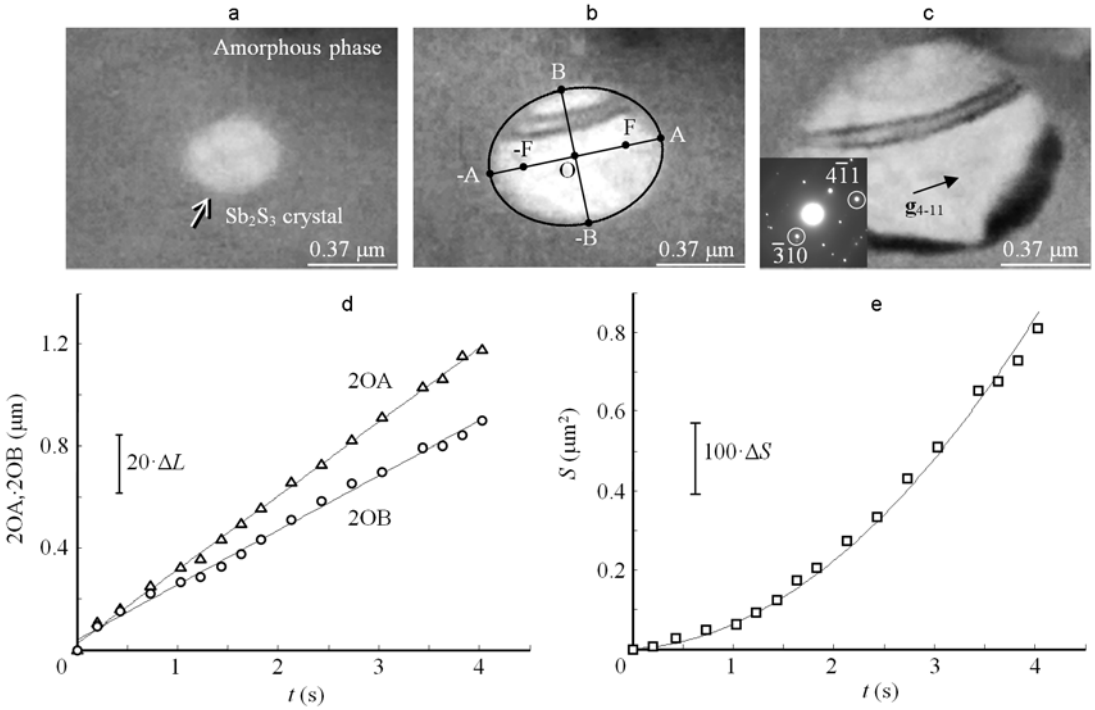

Fig. 1. Linear increase in crystal size during crystallization of an amorphous Sb_2S_3 film. Micrographs of the growing ellipse-shaped crystal at the time moment t after the start of video recording: (a) t = 1.23 s; (b) t = 2.13 s; (c) t = 3.63 s. Time dependences of the lengths of the major axis 2OA and minor axis 2OB of the crystal (d) and the area S of the crystal image (e). The solid line corresponds to the π·OA·OB product. Errors are ΔL = 0.012 μm, ΔS = 0.0018 μm^2.

1. Introduction

Antimony sulfide (Sb_2S_3) is a semiconductor with a layered orthorhombic crystal structure with parameters a_0 = 1.123 nm, b_0 = 1.131 nm and c_0 = 0.3841 nm [1, 2]. The increased interest in Sb_2S_3 films in crystalline and amorphous state is due to their many useful physical properties. In particular, Sb_2S_3 is widely used in microwave devices, optoelectronic devices and solar cell absorbers [3]. Antimony sulfide films deposited on a substrate at room temperature are amorphous [4]. Post-condensation annealing of the films (160–300°C) initiates their crystallization accompanied with a change in the physical properties of Sb_2S_3 [5].

Amorphous films of Sb_2S_3 can crystallize under the action of an electron beam. This can be performed in a transmission electron microscope (TEM) using the so-called *in situ* method [4]. This method was used in [4] to study the structure and morphology of crystals growing in an amorphous Sb_2S_3 film with a slight excess of antimony. According to [4], electron beam irradiation of amorphous non-stoichiometric films with an excess of antimony initiates the predominant crystallization [6] of Sb during the first stage of the process, and subsequent matrix Sb_2S_3 crystallization during the second stage. At present, there are no detailed data on the kinetics and morphology of crystal growth during polymorphous [6] electron-beam crystallization of amorphous films. The purpose of this work was to study the kinetics and morphology of crystal growth during the polymorphous electron-beam crystallization of amorphous Sb_2S_3films. TEM with video recording *in situ* of the number and size of crystals growing in the amorphous film makes it possible to do this.

2. Experimental

Amorphous Sb_2S_3 films were grown on the (001) face of KCl single crystals at room temperature by thermal evaporation in a vacuum chamber (~ 10^{-6} Torr). The thickness h of the films varied in the range from 25 to 35 nm. The evaporation was carried out by rapidly heating the tantalum crucible by passing a pulse of electric current. To preserve the stoichiometric composition of the amorphous phase, a mixture of Sb_2S_3 powder with the addition of S powder (~ 4 wt. %) was used. Films were separated

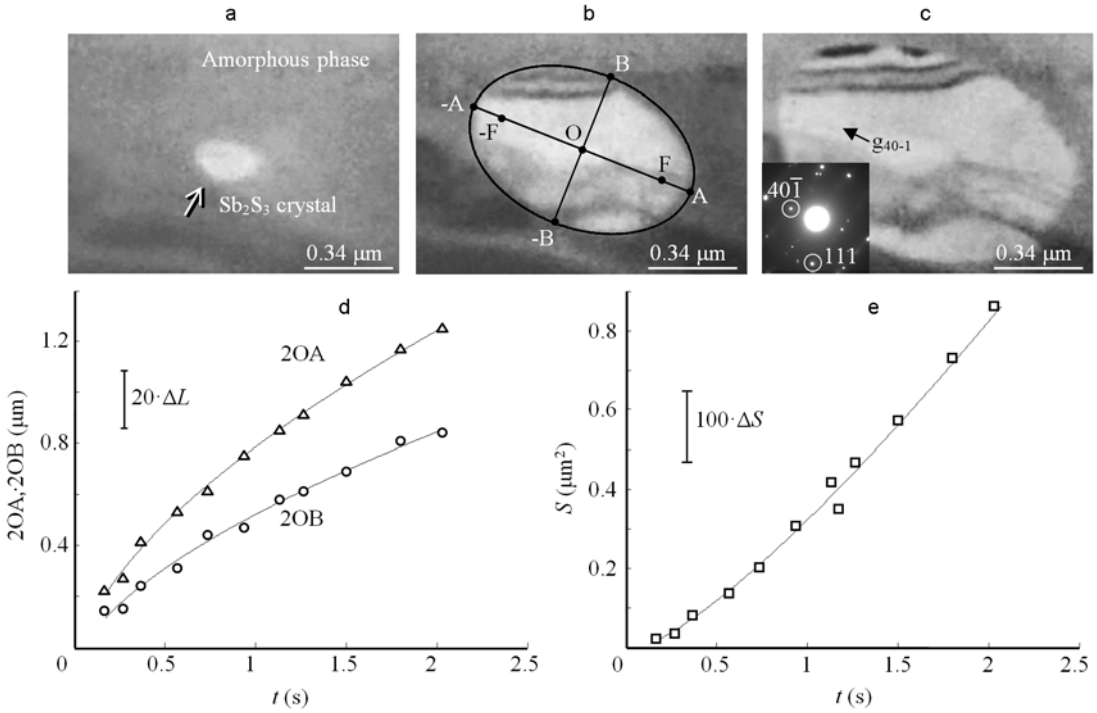

Fig. 2. Nonlinear increase in crystal size during crystallization of an amorphous Sb_2S_3 film. Micrographs of the growing ellipse-shaped crystal at the time moment t after the start of video recording:: (a) $t = 0.27$ s; (b) $t = 1.27$ s; (c) $t = 2.03$ s. Time dependences of the lengths of the major axis 2OA and minor axis 2OB of the crystal (d) and the area S of the crystal image (e). The solid line corresponds to the π·OA·OB product. Errors are $\Delta L = 0.012$ μm, $\Delta S = 0.0018$ μm^2.

from the substrate in distilled water and transferred onto subject grids for electron microscopy studies. Phase transformations in the film were initiated with electron beam irradiation, and the rate of crystallization was controlled by varying the density of the electron current through the sample. The crystallization process was recorded with a movie camera [7] from a microscope screen with a frame rate of 30 s^{-1}. The size and area of crystals was determined from their electron microscopic images using a specialized computer program. When determining the error, the image quality of microparticles in the electron microscopic video was taken into account. The error in measuring the length ΔL was 0.012 μm, and the error in measuring the area was $\Delta S = 0.0018$ μm^2.

3. Results and discussion

Fig. 1 illustrates the crystallization of an amorphous Sb_2S_3 film. Electron microscopic photographs correspond to the moments of time t that have passed after the start of video recording: (a) $t = 1.23$ s; (b) $t = 2.13$ s; (c) $t = 3.63$ s. According to this video, an ellipse-shaped Sb_2S_3 crystal grows in an amorphous matrix as long as the film is exposed to the electron beam. The time dependences of the lengths of the major axis 2OA and minor axis 2OB of the ellipse-shaped Sb_2S_3 crystal are shown in Fig. 1d. The straight lines were plotted by the experimental length values using the least-squares technique. Linear dependences were observed:

$$2OA = 0.290t + 0.023\mu m, \qquad (1a)$$

$$2OB = 0.215t + 0.038\mu m\ , \qquad (1b)$$

where t is measured in seconds. According to Eq. (1a), the growth rate of the major axis 2OA (tangent of the slope of the straight line to the abscissa axis) is $v_{2OA} = 0.290$ μm·s^{-1}. The growth rate of the minor axis 2OB is $v_{2OB} = 0.215$ μm·s^{-1}.

The time dependence of the area S of the image of an ellipse-shaped Sb_2S_3 crystal is shown in Fig. 1e. The experimental data are satisfactorily described by the function $S = \pi$·OA·OB, which specifies the area of the ellipse (the solid line). According to (1a) and (1b), the dependence $S(t)$ corresponds to a polynomial of the second power in t.

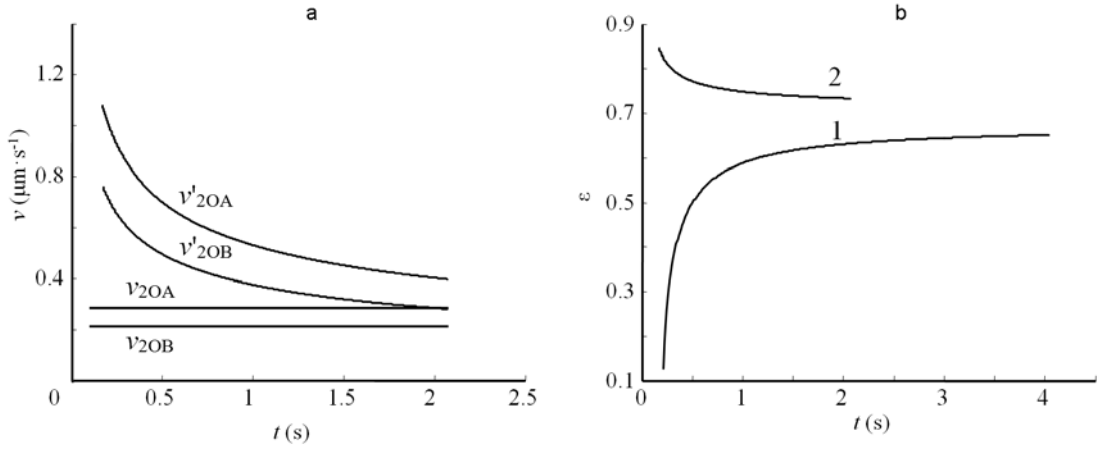

Fig. 3. a) Time dependences of the growth rate ν of the major axis 2OA and minor axis 2OB of an ellipse-shaped Sb_2S_3 crystal in the cases of a linear (ν_{2OA} and ν_{2OB}) and nonlinear (ν'_{2OA} and ν'_{2OB}) increase in the size of the crystal. b) Time dependences of the eccentricity ε of an ellipse-shaped crystal in the cases of linear (*1*) and nonlinear (*2*) crystal size increase.

Fig. 2 illustrates a variant of polymorphous crystallization of an amorphous Sb_2S_3 film, when a nonlinear time dependence of the crystal size is realized. Electron microphotographs correspond to the periods of time t that have passed after the start of video recording: (a) $t = 0.27$ s; (b) $t = 1.27$ s; (c) $t = 2.03$ s. The time dependences of the lengths of the major axis 2OA and minor axis 2OB of the ellipse-shaped Sb_2S_3 crystal are shown in Fig. 2d. Nonlinear dependences are observed:

$$2OA = 0.885t^{0.6} - 0.101\mu m, \qquad (2a)$$

$$2OB = 0.626t^{0.6} - 0.107\mu m. \qquad (2b)$$

The absence of precipitation of microcrystalline antimony particles (Fig. 1 and Fig. 2) indicates that according to the classification scheme [6], the crystallization is polymorphous. The amorphous film becomes crystalline without changing the composition. When the dependence $S(t)$ corresponds to a polynomial of the second power, then according to (1a) and (1b), the growth rates ν_{2OA} and ν_{2OB} are constant. Otherwise, according to (2a) and (2b), the growth rates ν'_{2OA} and ν'_{2OB} are not constant, but decrease with time (Fig. 3a).

The numerical characteristic of the ellipse, showing the degree of its deviation from the circle, is the eccentricity ε:

$$\varepsilon = \sqrt{1 - \left(\frac{OB}{OA}\right)^2}, \qquad (3)$$

For an ellipse-shaped Sb_2S_3 crystal, we can obtain the time dependence of ε by substituting relations (1a, b) or (2a, b) into formula (3). The result is shown in Fig. 3b. In the case of a linear increase in the crystal size, the eccentricity monotonically increases with time (line 1). Therefore, as the crystal grows, it stretches. Otherwise, in the case of a nonlinear increase in the crystal size, the eccentricity monotonically decreases with time (line 2). Therefore, as the crystal grows, it becomes rounder.

According to video recording data (Fig. 1, Fig. 2), during polymorphous crystallization of an amorphous Sb_2S_3 film, a single ellipse-shaped Sb_2S_3 crystal grows in the field of observation. This is the main qualitative feature of layer polymorphous crystallization (LPC) [8]. A quantitative feature of LPC is the value of the relative length δ_0 [9] determined as

$$\delta_0 = \frac{D_0}{a_0}, \qquad (4)$$

where a_0 is the cell parameter of the growing crystal. D_0 is the characteristic unit of length. According to [10], D_0 is the average crystal size at the time $t = t_0$ (t_0 is characteristic unit of time), after which the volume of the amorphous phase decreases by a factor of $e = 2.718$. At this moment, the fraction of the crystalline phase $x = 0.632$. A simple relation connects D_0 and t_0:

$$D_0 = \langle \nu_\tau \rangle t_0, \qquad (5)$$

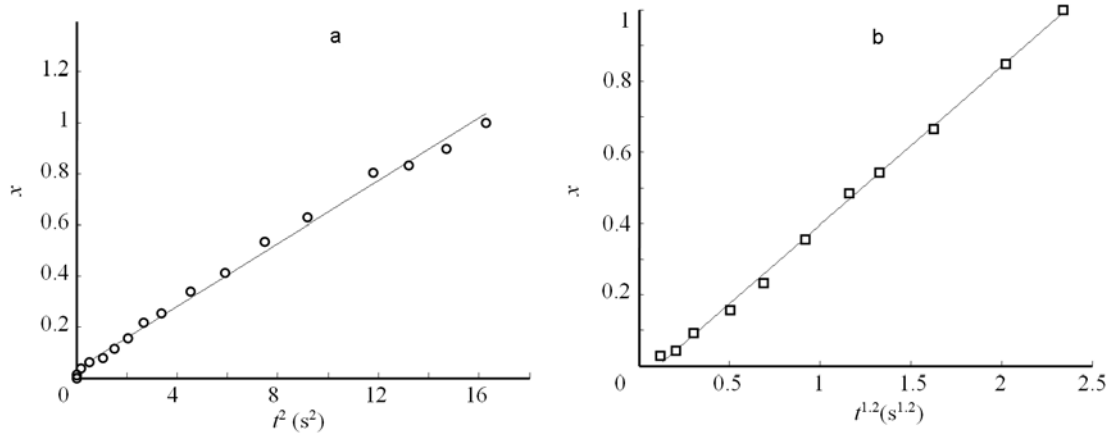

Fig. 4. Time dependences of the crystallized fraction $x(t)$ in the case of a linear increase in the crystal size (a) and in the case of a nonlinear increase in the crystal size (b) during crystallization of amorphous Sb_2S_3 film.

where $<\nu_\tau>$ is the average tangential growth rate of crystals in the amorphous film.

To use relation (4), we must determine quantities analogous to D_0 and a_0, taking into account the shapes and orientations of Sb_2S_3 crystals at the final stage of their growth. In turn, this requires knowledge of the dependence of the fraction of the crystalline phase x on time t. In the case of LPC, when one crystal grows in the observation field, we can define $x(t)$ as the ratio of the crystal area $S(t)$ at time t to the crystal area S_0 at the last frame of the electron microscope video:

$$x(t) = \frac{S(t)}{S_0}. \qquad (6)$$

For the case of a linear increase in the crystal size (Fig. 1) and $S_0 = 0.81$ μm^2, the dependence $x(t)$ in coordinates of $x - t^2$ is presented in Fig. 4a. Its analytical dependence has the form:

$$x = 0.062t^2 + 0.030. \qquad (7)$$

According to (7), the value $x = 0.632$ corresponds to the characteristic time $t = t_0 = 3.116$ s. Substituting this value to (5) for $<\nu_\tau> = \nu_{2OA} = 0.290$ μm·s^{-1} we get $D_0 = 0.904$ μm. The SAED pattern of the Sb_2S_3 crystal (Fig. 1c) sets the position of the diffraction vector $\mathbf{g}_{4\text{-}11}$. In this direction, the major axis 2OA of the ellipse-shaped Sb_2S_3 crystal increases. This is done by attaching of (411) planes with the interplanar distance $d_{4\text{-}11} = 0.2222$ nm. Then, according to (4), using $d_{4\text{-}11}$ instead of a_0, we get the relative length $\delta_0 \approx 4068$.

For the case of a nonlinear increase in the crystal size (Fig. 2) and $S_0 = 0.86$ μm^2, the dependence $x(t)$ in coordinates of $x - t^{1.2}$ is presented in Fig. 4b. Its analytical dependence has the form:

$$x = 0.443t^{1.2} - 0.048. \qquad (8)$$

According to (8), the value $x = 0.632$ corresponds to the characteristic time $t = t_0 = 1.429$ s. At this moment t_0 according to (2a), the velocity $<\nu_\tau> = \nu'_{2OA} = 0.460$ μm·s^{-1} (Fig. 3a). Substituting this value to (5) we get $D_0 = 0.657$ μm. The SAED pattern of the Sb_2S_3 crystal (Fig. 2c) sets the position of the diffraction vector $\mathbf{g}_{40\text{-}1}$. In this direction, the major axis 2OA of the ellipse-shaped Sb_2S_3 crystal increases. This is done by attaching of $(40\bar{1})$ planes with the interplanar distance $d_{40\text{-}1} = 0.2267$ nm. Then, according to (4), using $d_{40\text{-}1}$ instead of a_0, we get the relative length $\delta_0 \approx 2898$.

4. Conclusions

Electron beam irradiation of an amorphous Sb_2S_3 film with stoichiometric composition causes a phase transformation according to the scheme of layer polymorphous crystallization. A single planar ellipse-shaped Sb_2S_3 crystal nucleates and grows in the observed region of the film. The time dependences of the lengths of major and minor ellipse axis of crystal can be both linear and non-linear. In the linear case, the time dependences of the ellipse-shaped crystal area S and the crystallized fraction x are quadratic. Wherein the relative length $\delta_0 \approx 4068$. As the ellipse-shaped

crystal grows, its eccentricity monotonically increases with time; that corresponds to an increase in its elongation along the major axis.

In the case of a nonlinear increase in the crystal size, the time dependences of the ellipse-shaped crystal area S and the crystallized fraction x can be described by a power function with the exponent of 1.2. Wherein the relative length $\delta_0 \approx 2898$. As the ellipse-shaped crystal grows, its eccentricity decreases monotonically with time. This corresponds to a decrease in its elongation along the major axis.

δ_0 values of several thousand (as in the case of Sb_2S_3) are typical for layer-by-layer polymorphous crystallization of amorphous substances (for example, Cr_2O_3, V_2O_3), when a single crystal layer is formed. The formation of a polycrystalline film during island polymorphous crystallization corresponds to δ_0 values of several hundred (for example, $\delta_0 = 100$ for ion-plasma deposition of an amorphous ZrO_2 film and $\delta_0 = 805$ for laser deposition of an amorphous ZrO_2 film) [9].

The observed difference in the kinetics and morphology of crystal growth within the framework of layer polymorphic crystallization can be explained by local microinhomogeneities of the film, formed by thermal evaporation of the charge. In this case, the phenomenon of polyamorphism appears in amorphous structures. According to [11], in amorphous films of the same composition, the existence of two or more forms with different short-range order of the arrangement of atoms in the first coordination sphere is possible. In amorphous films, the kinetics of crystallization of areas with different short-range orders is different.

References

1. I.S.Virt, I.O.Rudyj, I.V.Kurilo et al., *Semiconductors*, **47**, 1003 (2013).
2. JCPDS Powder Diffraction File Card No. 42-1393 (International Centre for Diffraction Data, Swarthmore, PA (1996).
3. M.Trivedi, G.Nayak, S.Patil et al., *Ind.Eng. Manage*, **4**, 1 (2015).
4. A.G.Bagmut, S.N.Grigorov, V.M.Kosevich et al., *Functional Materials*, **15**, 332 (2008).
5. S.Mahanty, J.M.Merino, M.Lerona, *J.Vac.Sci. Technol.*, **A 15**, 3060 (1997).
6. U.Koster, U.Herold, Crystallization of Metallic Glasses, in: H.-J.Guntherodt, H.Beck (Eds.), Glassy Metals i Ionic Structure, Electronic Transport, and Crystallization, Springer, Berlin Heidelberg, New York (1981), p.225.
7. A.G.Bagmut, I.A.Bagmut, *Mol.Cryst.Liquid Cryst.*, **673**, 120 (2018).
8. A.G.Bagmut, *Tech.Phys.Lett.*, **38**, 488 (2012).
9. A.G.Bagmut, *Functional Materials*, **26**, 6 (2019).
10. A.N.Kolmogorov, *Izv.Acad.Sci.USSR, Ser. Math.*, **1**, 355 (1937).
11. L.S.Palatnik, A.A.Nechitailo, A.A.Kozma, *Dokl.Akad.Nauk SSSR*, **261**, 1134 (1981).